JOURNAL OF MATERIALS SCIENCE 3 (1968) 150–157

The Sintering of Nickel/Aluminium Spheres to Nickel Plates*

A. G. ELLIOT†, Z. A. MUNIR‡
Department of Materials Science, San Jose State College, California, USA

Received 10 July 1967, and in revised form 6 November

Spheres of nickel, and of nickel containing 0.5, 1.0, 2.0, and 10.0 wt % aluminium, all of approximately 100 μm diameter, were sintered under vacuum to nickel plates for various times within the temperature range 1000 to 1300° C. Neck growth was determined as a function of time. Values for the exponent of time in the neck growth equation, $x/a = At^n$, of 0.19, 0.18, 0.15, and 0.16 were found for the above compositions, respectively. An activation energy of 33 kcal/mole was found for sintering nickel spheres to nickel plates. An activation energy of 69 kcal/mole was found for sintering Ni/1.0% Al spheres to nickel plates.

Assuming a surface-diffusion mechanism of material transport, as suggested by Nichols and Mullins, the difference in activation energies is explained on the basis of a difference in surface energy, as reflected in the ease with which vacancies are formed at the surface. Similar reasoning is employed to explain the difference in activation energies found between sintering nickel spheres to nickel plates under vacuum in this research, and sintering nickel wire compacts under a hydrogen atmosphere in work reported by Pranatis and Siegle.

1. Introduction

The sintering of a sphere to a plate was used by Kuczynski [1] as a model in his analysis of sintering mechanisms. In such a model the difference in the vacancy concentration between the neck area and the bulk of the material is the driving force for mass transport into the neck region. The presence of a compositional concentration gradient, however, may mask the vacancy concentration gradient, and as shown by Stablein and Kuczynski [2], mass transport due to a compositional concentration gradient occurs first. Sintering forces can become active only when this concentration gradient has vanished. In alloys where the relative diffusivities of the species involved are about the same, the effects of alloying may manifest themselves in several forms: a change in the sintering mechanism, sintering rate, and/or activation energy for the sintering process.

No analysis has been made of the effects of either minor alloying additions or of composition gradients on the kinetics of sintering. This work deals with such an analysis using dilute solutions of aluminium in nickel.

2. Experimental Methods

Nickel/aluminium alloys in the α solid solution region were prepared by melting mixed elemental powders having compositions of 0.5, 1.0, 2.0 and 10.0 wt % aluminium. Nickel powder, having a 99.96% purity, and 99.99% pure aluminium were mixed and melted under a vacuum of 10^{-5} torr in high purity alumina crucibles. The melt was homogenised near 1500° C for at least 15 min.

*From the thesis submitted by A. G. Elliot in partial fulfilment of the requirements of the degree of Master of Science in Materials Science.

†Current address: The Lockheed Missiles and Space Company, Palo Alto, California, USA
‡Current address: School of Engineering Science, The Florida State University, Tallahassee, Florida, USA

Filings obtained from the resulting solid ingots were sieved, and the <100 to >90 μm size fraction retained for spheroidising. The <90 μm size fraction was retained for subsequent X-ray diffraction analysis.

An X-ray analysis of the ingot filings was performed to ensure that alloying had taken place. The filings were annealed in a hydrogen atmosphere for 12 h at 600° C to remove residual stresses. Debye-Scherrer powder photographs were then made, from which lattice parameter measurements were obtained.

The filings were spheroidised by passing them down through an induction-heated, vertical-tube furnace. The furnace consisted of a graphite susceptor 2.5 cm OD by 1.9 cm ID by 15.2 cm long, wrapped with graphite cloth insulation, and contained in a 4.7 cm ID water-cooled, double-walled glass tube. A gas mixture of argon with 0.25% H_2 was used to provide a reducing atmosphere, thus keeping the possibility of oxidation of the particles to a minimum. An alumina tube down the centre of the furnace ensured against loss of material due to reaction with the susceptor wall. Wall temperatures of 1750 to 1800° C, as measured with a Leeds and Northrop disappearing-filament optical pyrometer, were found necessary for effective spheroidisation.

The spherical particles were separated from the non-spherical particles by rolling them down a smooth-surfaced, slightly inclined plane. These particles were then sieved and the <100 to >90 μm size fraction retained for the sintering experiments.

Spherical nickel powder, −150 to +200 mesh, prepared by an atomisation process, was used as the control material. Nearly perfect spherical particles were selected in the same manner as that described above.

Plates were prepared from 0.05 cm thick nickel strip with a purity of 99.98% nickel-plus-cobalt. Washers which were cut from a 0.63 cm diameter nickel tube, smoothed down on one face, and spot welded to the nickel plates, were used to contain the spheres on the nickel plate. These plates were electropolished in a solution of 23 vol % perchloric acid and 77 vol % glacial acetic acid, to remove surface contamination. They were then annealed in vacuum for at least 30 min at about 1300° C to remove residual stresses. The spherical particles were then dispersed over this prepared surface and sintered.

Sintering was carried out under vacuum in the pressure range of 10^{-5} torr in a cold-wall, resistance-heated furnace employing a molybdenum wire heating element and molybdenum sheet radiation shields. Alumina boats were used to contain the samples.

Temperatures were measured with the Leeds and Northrop disappearing-filament optical pyrometer. The brightness temperature of the alumina surface was used as a reference temperature. The system was calibrated by measuring the alumina surface brightness temperature at the melting points of copper, nickel, and platinum. Temperature control was exercised manually through adjustment of a Variac. Temperatures were controlled and reproduced to within ±15° C for each experimental sintering run.

Spheres of pure nickel and nickel with 0.5, 1.0, 2.0, and 10.0 wt % aluminium were sintered to the nickel plates at 1000 and 1300° C for various lengths of time. In addition, spheres of nickel and nickel with 0.5, 1.0, and 2.0% aluminium were sintered to nickel plates for 120 min at 1200° C, and spheres of nickel and nickel with 1.0% aluminium were sintered to nickel plates for 120 min at 1100° C.

Samples of various compositions were sintered simultaneously for each given time period at a particular temperature. The samples could be brought to temperature within 2 to 3 min.

Analysis of each of the sintered samples consisted of (i) measurements of the diameters of a number of spheres, and (ii) measurements of the diameters of a number of the necks formed between the spheres and the plate. In order to obtain a reliable average value of sphere diameters, between ten and thirty measurements were made on each sample run. A minimum of twenty neck diameters were measured on each sample, from which an average value was obtained, and a standard deviation calculated. Sphere and neck diameter measurements were made utilising a Zeiss metallograph. As one approach, groups of from five to ten spheres were photographed at 285× magnification, and diameter measurements were made on the photographs. This gave an accuracy of ±2 μm (±2%) in the measured sphere diameters. The spheres were also measured directly utilising a filar eyepiece calibrated against a millimeter scale having 0.01 mm divisions. This method gave a measuring accuracy of ±2 μm also. After sphere diameter measurements were

obtained, the spheres were swept off the surface of the plates to reveal the cross sections of the necks. These were measured directly utilising the filar eyepiece. The cross sections of the necks were generally irregular. This was compensated for by obtaining measurements in random directions. The neck diameters were measured with an accuracy of ± 0.5 μm ($\pm 2\%$).

3. Experimental Results

Results of the sphere diameter measurements are summarised in table I.

TABLE I Results of sphere diameter measurements.

System	Total number of spheres measured	Average sphere diameter (μm)
Unalloyed Ni	119	96
Ni/0.5% Al	136	102
Ni/1.0% Al	152	100
Ni/2.0% Al	228	94
Ni/10.0% Al	121	96

Neck growth in the unalloyed nickel system is represented by the graph in fig. 1. The slopes of the best-fit straight lines for the data points at 1000 and 1300° C are 0.19 and 0.17, respectively. These values were obtained by a least squares analysis of the data, using an equation of the form $\log x/a = \log A + n \log t$, where x is the neck radius, a is the sphere radius, t is time, and A and n are constants.

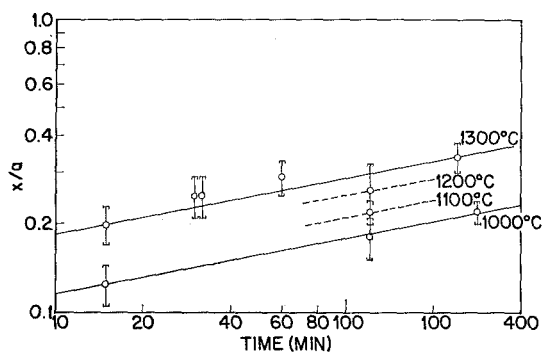

Figure 1 Neck growth for nickel spheres on nickel plates at various temperatures.

Neck growth in the aluminium alloyed systems depended strongly on concentration. Neck growth in the Ni/0.5% Al and Ni/1.0% Al systems is shown in fig. 2. The best-fit straight lines through the 1300° C data points by least squares analysis give slopes of 0.16 and 0.20, respectively. Neck growth in the Ni/2.0% Al and Ni/10.0% Al alloy systems are shown in fig. 3. Least squares analysis gives slopes of 0.11 and 0.16, respectively.

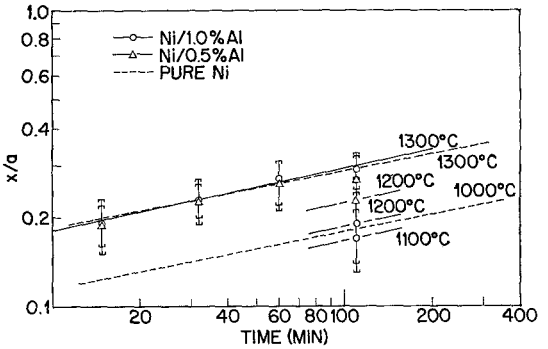

Figure 2 Neck growth for aluminium alloyed nickel (Ni/0.5 and 1.0% Al) at various temperatures.

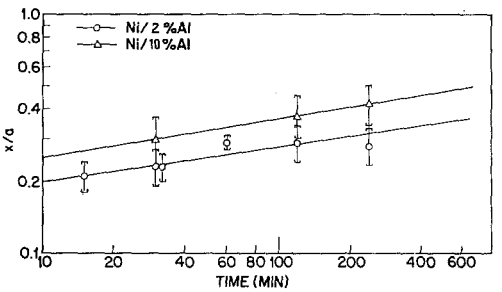

Figure 3 Neck growth for aluminium alloyed nickel (Ni/2.0 and 10.0% Al) at 1300° C.

Neck formation in the aluminium alloyed systems was negligible at 1000° C for sintering times up to 120 min. Most of the spheres did not become attached to the plates, except in a few isolated cases. In one specific case, the Ni/0.5% Al system, measurement was obtained directly on a sphere and its associated neck.

During the course of making measurements, several interesting phenomena were observed. Thermal faceting of the nickel plate surface was quite prominent, especially after 4 h at 1300° C. This effect was severely altered in the presence of aluminium alloyed spheres, primarily by those having high aluminium content. The necks formed between the nickel/aluminium alloy spheres and the nickel plate were brittle and weak, whereas those between the nickel spheres and the nickel plate were quite strong. This was evidenced by the ease with which the alloyed spheres could be swept away for neck diameter measurements, compared to the difficulty experienced in removing the unalloyed spheres. Also, the high aluminium alloy sphere

necks generally broke at a height above the surface of the plate, whereas the pure nickel spheres broke off quite close to the plate surface.

X-ray analysis of the nickel powder used to fabricate the nickel/aluminium alloys indicated the presence of cobalt oxides, nickel oxides, and/or solid solutions thereof. X-ray analysis of the alloy ingots also showed the same materials present and to the same degree. However, an electron beam microprobe analysis of an Ni/10.0% Al alloy sintered for 120 min at 1300° C showed the presence of only nickel and aluminium. Non-homogeneous compositions for both the Ni/2.0% Al and Ni/10.0% Al alloys were indicated by broad diffuse bands occurring in the back reflection region where normally "$K_{\alpha 1}$-$K_{\alpha 2}$" doublets are resolved. No X-ray evidence for the existence of Ni_3Al was found in any but the Ni/10.0% Al spheres.

An examination of the microstructures of the cross sections from the sphere through the neck into the plate revealed little of interest except in the Ni/10.0% Al alloy system. Fig. 4 shows a photomicrograph taken at a section through the neck, typical of the sample sintered 120 min at 1300° C. A shell of second-phase Ni_3Al material has precipitated near the surface of the sphere. Small particles of second-phase material, and void areas, are present within the interior of the sphere. Grooving of the surface of the plate near the neck has occurred, as well as the formation of voids in the plate directly beneath the neck. A few oxide inclusions are present in this as well as in some of the other spheres, as indicated by their distinct glassy appearance under the microscope.

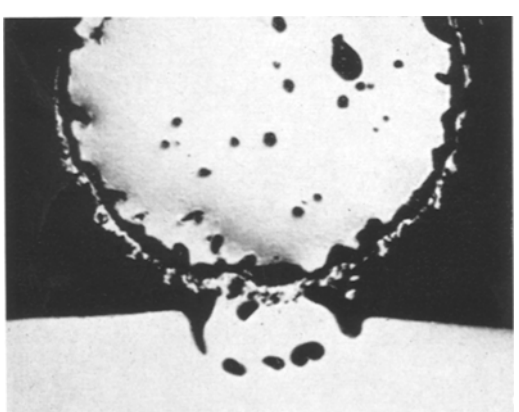

Figure 4 Photomicrograph at a Ni/10.0% Al alloy sphere sintered to a nickel plate for 120 min at 1300° C. Unetched, ×535.

4. Discussion

4.1. Reliability of Data

The standard deviations of the x/a measurements are shown by the brackets in figs. 1, 2 and 3. These deviations are of the order of 10 to 15%. Such magnitudes are due to (i) the distribution in sphere sizes, (ii) non-homogeneities in composition (e.g., Ni/2.0 and 10.0% Al), (iii) to sphere surface irregularities producing non-circular necks, and (iv) to normal statistical variations. Wilson and Shewmon [3] pointed out that a 20% variation in x/a values is to be expected for a given set of sintering conditions and spheres of identical diameter.

Because of the statistical approach used in determining x/a ratios, effects due to inhomogeneities in composition were not excluded. The results of these are noticeable for the Ni/2.0% Al system where the scatter in the data is relatively wide. It is improbable, however, that inhomogeneity effects should cause variations greater than the expected 20%. The lack of such effects in the Ni/10.0% Al system may be attributed to the precipitation of the Ni_3Al shell in the spheres as mentioned earlier.

The presence of cobalt oxide impurities had no ultimate effect upon the sintering of the alloy systems. These oxides agglomerated during alloy formation and subsequent spheroidisation, such that they could be observed under the microscope. The oxides had the effect of tying up the impurities, since no trace contaminants in the bulk of the spheres were revealed by microprobe analysis.

4.2. Neck Growth in the Pure Nickel System

The time-dependent necks growth equations as determined from the isothermal log/log plots of figs. 1, 2 and 3 are summarised in table II. The value for the exponent in the case of the unalloyed nickel control material is in complete agreement with values reported by Pranatis and Siegle [4] for sintering nickel wire compacts. According to theory, these values of the exponent, approximately 1/5, indicate either volume or grain boundary diffusion as the operative material transport mechanism. Pranatis and Siegle [4] postulated a volume-diffusion mechanism based on their observation of a lack of an effect on neck growth of the presence or absence of grain boundaries, their analysis of void disappearance, and the proximity to values reported in the literature of their calculated values for self-

diffusion coefficients and the activation energy for diffusion. Further, they found agreement with Herring's scaling laws [5] for a volume-diffusion mechanism.

TABLE II Summary of neck growth equations.

System	Neck growth as a function of time
Pure Ni 1000° C	$x/a = A_1 t^{0.19}$
Pure Ni 1300° C	$x/a = A_1 t^{0.17}$
Ni/0.5% Al	$x/a = A_2 t^{0.16}$
Ni/1.0% Al	$x/a = A_3 t^{0.20}$
Ni/2.0% Al	$x/a = A_4 t^{0.11}$
Ni/10.0% Al	$x/a = A_5 t^{0.16}$

In order to relate more closely the results of this investigation with those of Pranatis and Siegle, steps were taken to obtain rate constants and an associated activation energy for diffusion. The data of fig. 1 were replotted in fig. 5 as x/a versus $t^{0.19}$. Best-fit straight lines were drawn from the origin through the data points. From the slopes of these lines, values were obtained for A_1 as a function of temperature. The value for the 1000 and 1300° C data points was determined precisely by the least squares analysis of the data mentioned earlier. All of these values are shown in table III. Only one point was obtained at each of the temperatures

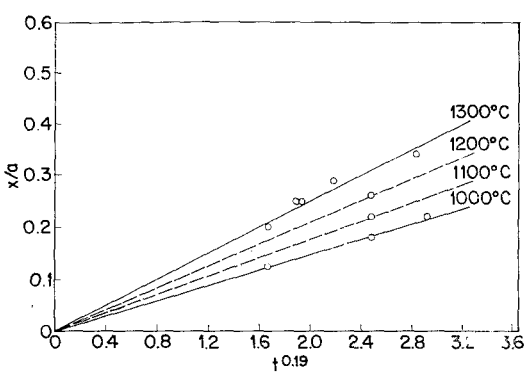

Figure 5 Kinetics of neck growth for pure nickel spheres on nickel plates.

1100 and 1200° C, which, it was assumed, uniquely determined the value of A_1 at that temperature. The inclusion of these values for the ultimate quantitative determination of an activation energy is rather tenuous. However, as shown in an Arrhenius plot to be discussed below, the proximity of the resulting rate constants to the straight line connecting the more firmly established values at 1000 and 1300° C justifies their use.

Using Kuczynski's [1] analysis for a volume-diffusion mechanism, the rate constant for sintering will be related to A by $K^{1/5} = A$. Thus, a plot of the logarithm of the fifth power of the experimentally determined A values versus $1/T$ should give a straight line whose slope is $-Q/R$, where Q is the activation energy for diffusion and R is the gas constant. Such a plot of table III results is shown in fig. 6. An activation energy of 33 kcal/mole was obtained by a least squares analysis for the sintering of ~100 μm diameter pure nickel spheres to nickel plates in vacuum. Also included are the data from Pranatis and Siegle for their 160 μm diameter wire compacts which they sintered in a hydrogen atmosphere. They obtained an activation energy of 80 kcal/mole as compared to approximately 69 kcal/mole for the self-diffusion of nickel determined by other means [6, 7]. It is interesting to note that, when a grain boundary diffusion mechanism is assumed, a value for the activation energy of 26 kcal/mole is obtained [8, 9].

The direct comparison of activation energies determined from sintering experiments with those determined by other means, much less the direct comparison of diffusion coefficients, is open to serious question. Recent work by Nichols and Mullins [10], and Wilson and Shewmon [3] indicates that surface-diffusion should be the predominant material transport mechanism in the sintering of spheres to plates. The former point out that the exponent of the time-dependent neck growth equations should vary from

TABLE III Values for the neck growth equations constants.

System	Constant	Temperature (° C) 1000	1100	1200	1300
Pure Ni	A_1	0.0727	0.0846	0.100	0.137
	$(A_1)^5$	0.203×10^{-5}	0.433×10^{-5}	1.0×10^{-5}	4.84×10^{-5}
Ni/1.0% Al	A_3	0.0346	0.065	0.074	0.114
	$(A_3)^5$	0.005×10^{-5}	0.116×10^{-5}	0.222×10^{-5}	1.93×10^{-5}
Ni/2.0% Al	A_4	—	—	0.108	0.135
Ni/10.0% Al	A_5	—	—	—	0.178

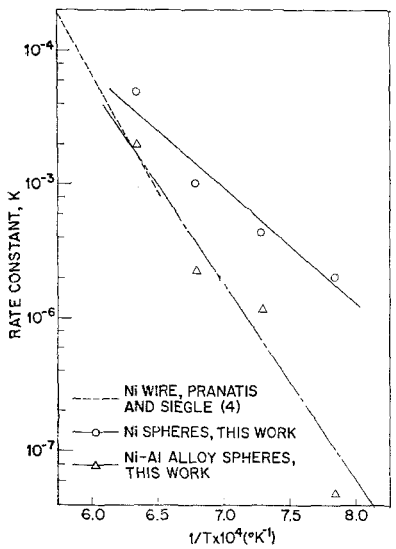

Figure 6 Rate constant versus $1/T$ for Ni and Ni/Al alloys.

1/5.6 to ~1/8 throughout the range $0.05 \leqslant x/a \leqslant 0.7$. These findings were based upon a precise mathematical analysis of the change in shape of the neck formed between a sphere and a plate due to the surface-diffusion alone. As a consequence, the tenuous assumptions in the original Kuczynski analysis were overcome, i.e. account was taken of the fact that the neck shape changes with time, with grooves being formed on both sides of the neck, and precise instead of approximate geometrical relations were obtained.

If one assumes that surface-diffusion is the operative material transport mechanism in the sintering of metallic systems, specifically nickel, then the difference in activation energy for the process observed between this research and that of Pranatis and Siegle may be rationalised in terms of surface energy, i.e. there should be no effect due to sample configuration. The latter work was carried out in a hydrogen atmosphere, whereas this work was done under vacuum (10^{-5} torr). Although a vacuum of this magnitude is not expected to produce absolutely clean surfaces, nevertheless, a significant difference in surface energy may exist under these two conditions. This is substantiated by the fact that the contact angle for liquid nickel on refractory substrates varies with the environment [11]. Such differences in surface energy may very well affect the energetics of vacancy formation, and thus lead to differences in the activation energy for sintering.

4.3. Neck Growth in the Aluminium Alloyed Nickel System

The addition of aluminium to form dilute alloy spheres (Ni/0.5% Al and 1.0% Al) had little effect on the kinetics of sintering at 1300° C as shown in fig. 2. Although a slope of 0.20 was obtained for the Ni/1.0% Al system, due to the large standard deviation, this could easily have been 0.19 or 0.18. Therefore, no alteration of the mechanism of material transport occurred. The kinetics of sintering at lower temperatures were definitely affected by the addition of 0.5 or 1.0% Al, however, as neck growth in these systems was much less than that in unalloyed nickel, with the difference becoming greater with decreasing temperature as indicated in fig. 2. This difference may indicate a significantly greater activation energy in the alloy systems.

The activation energy for sintering in the Ni/0.5% Al and 1.0% Al alloy systems may be estimated by following the procedures outlined above for the unalloyed nickel system. The data for the Ni/1.0% Al system in fig. 2 were replotted as x/a versus $t^{0.20}$ in fig. 7. The point at 1000° C is that due to the single x/a determination made on the Ni/0.5% Al system. Its use is justified by (i) an inability to distinguish between data due to Ni/0.5% Al and Ni/1.0% Al compositions at 1300° C, and (ii) the fact that necks generally did not form in the alloy systems when sintered at 1000° C. This, then, would be the highest x/a value one should expect for Ni/1.0% Al for this time and temperature. Values of the constant A_3 (see table II) as a function of temperature were determined from the slope of the best-fit straight lines through the data points and the origin. The values are given in table III. The value of A_3 at 1000° C is an upper limit.

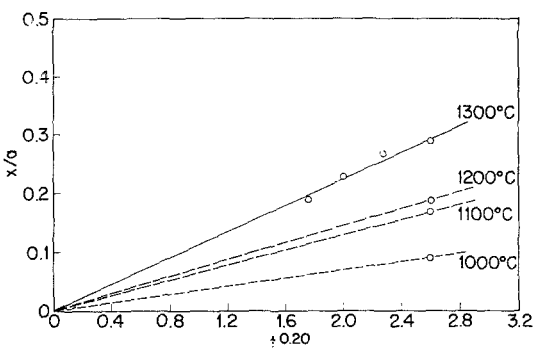

Figure 7 Kinetics of neck growth for Ni/1.0% alloys.

The activation energy was determined from the slope of a plot of log K versus $1/T$, $K = A^5$, given in fig. 6. A value of 69 kcal/mole was calculated by a least squares analysis of the data, and, based upon the discussion above, this value is a lower limit. This is a significant increase over the activation energy observed for pure nickel, though it is less than the value observed by Pranatis and Siegle for nickel sintered in hydrogen. A change in the surface energy due to alloying is quite plausible since the activity of nickel was changed sufficiently to allow the formation of intermetallics, e.g., Ni_3Al. Such a situation does not allow the solute activity gradient through the neck to be expressed simply in terms of a vacancy activity gradient since the solvent activity gradient through the neck is not negligible. Thus, any effect on sintering rate due to a composition gradient is masked by the change in activation energy due to alloying.

Additions of aluminium to the sphere in concentrations greater than 1.0% had effects more pronounced than those discussed above. As was previously indicated, the value of the exponent in the neck growth equation decreased significantly as shown in table II. The constants A_4 and A_5 for sintering of Ni/2.0% Al and Ni/10.0% Al respectively, were determined by computer analysis. These values are given in table III where it is observed that the neck growth rate constant has increased. These results are due to several causes. A significant cause in the Ni/2.0% Al system is inhomogeneity from sphere to sphere. Further, effects on surface phenomena were quite evident, which indicates that surface-diffusion played a prominent role in the transfer of material. According to the Kuczynski's treatment, the observed exponent for the neck growth equation is indicative of surface-diffusion as the primary material transport mechanism. However, based upon the findings of Nichols and Mullins [10], a straightforward interpretation is not evident.

An interesting aspect of the Ni/10.0% Al system is the occurrence of void areas beneath the neck surface as seen in fig. 4. The presence of these voids suggests the operation of a differential volume diffusivity between aluminium and nickel. Apparently nickel diffuses faster toward the centre of the sphere than does aluminium in the outward direction.

5. Conclusions

The initial stage sintering behaviour in vacuum of ~100 μm diameter nickel spheres to nickel plates is best described by a neck growth equation having the form $x/a = At^{0.19}$. An activation energy of 33 kcal/mole was calculated for the process. The exponent 0.19 in the neck growth equation is the same as that found by Pranatis and Siegle in their work on nickel wire compacts sintered under a hydrogen atmosphere. The activation energy found in this research, however, is half that found by Pranatis and Siegle. The 1/5 (approximately) power dependency of time in the neck growth equation suggests a volume-diffusion mechanism of material transport according to the Kuczynski analysis. This does not allow a rationalisation of the difference observed in activation energies between sintering in hydrogen and sintering in vacuum. If, however, as strongly suggested by Nichols and Mullins, a surface-diffusion mechanism is operative, then the observed difference in activation energy may be explained on the basis of a difference in surface energy as reflected in the ease with which vacancies may be formed at the surface.

The addition of up to 1.0% aluminium to the nickel spheres sintered to the nickel plates does not alter significantly the time-dependency of the neck growth equations. However, the calculated activation energy was found to be 69 kcal/mole which is significantly larger than that of pure Ni. The change in activation energy may be explained in terms of a change in surface energy provided a surface-diffusion mechanism is at least partially operative.

The addition of 2.0% aluminium to the nickel spheres decreased the value of the exponent for the time dependency of neck growth to 0.11. The neck growth rate constant at 1300° C was increased over that for Ni/1.0% Al. The value of the exponent corresponds to a predominantly surface-diffusion mechanism of material transport according to the Kuczynski approach. No interpretation was found in terms of the Nichols and Mullins approach.

A 10.0% aluminium addition to the nickel spheres resulted in precipitation of a shell of Ni_3Al near the surface of the sphere during spheroidisation. This altered the diffusion flux path such that both surface-diffusion and volume-diffusion contributed to neck growth. It was observed that nickel diffused faster through

the Ni_3Al shell than did aluminium. A value of 0.16 was found for the power dependency of time for neck growth. This system gave the largest neck diameters at 1300° C.

Acknowledgements

The authors are grateful to the Lockheed Missiles and Space Co* for their support of this work. The assistance of K. L. Berney and E. A. Carlton in the preparation of the manuscript is acknowledged.

References

1. C. G. KUCZYNSKI, *Trans. AIME* **185** (1949) 169.
2. (a) P. F. STABLEIN, JR and G. C. KUCZYNSKI, Proceedings of the Fourth International Symposium on Reactivity of Solids, Amsterdam (Elsevier, Amsterdam, 1960) p. 91.
   (b) P. G. STABLEIN, JR and G. C. KUCZYNSKI, *Acta Met.* **11** (1963) 1327.
3. T. L. WILSON and P. G. SHEWMON, *Trans. AIME* **236** (1966) 48.
4. A. L. PRANATIS and L. L. SIEGLE, "Powder Metallurgy", edited by W. Leszynski (Interscience, New York, 1961).
5. C. HERRING, *J. Appl. Phys.* **21** (1950) 301.
6. R. E. HUFFMAN, F. W. PIKUS, and R. A. WARD, *Trans. AIME* **206** (1955) 483.
7. A. MESSNER, R. BENSON, and J. DORN, ASM Preprint No. 193 (1960); *Met. Prog.* **78** (1960) 242.
8. W. R. UPTHEGROVE and M. J. SINNOTT, *Trans. Amer. Soc. Metals* **50** (1958) 1031.
9. W. LANGE, A. HASSNER, and G. MISCHER, *Phys. Status Solidi* **5** (1964) 63.
10. F. A. NICHOLS and W. W. MULLINS, *J. Appl. Phys.* **36** (1965) 1826.
11. M. HUMENIK, JR and W. D. KINGERY, *J. Amer. Ceram. Soc.* **37** (1954) 18.

*Address: Palo Alto, California, USA